

X-ray photoelectron spectroscopy studies of chromium compounds

M. C. Biesinger,^{1*} C. Brown,² J. R. Mycroft,² R. D. Davidson¹ and N. S. McIntyre¹

¹ Surface Science Western, Room G1, Western Science Centre, University of Western Ontario, London, Ontario, N6A 5B7, Canada

² Dofasco Inc., 1330 Burlington Street East, Hamilton, Ontario, L8N 3J5, Canada

Received 19 April 2004; Revised 1 July 2004; Accepted 19 July 2004

Photoelectron spectra of a number of chromium oxides and other compounds were studied under high spectral resolution conditions chosen to reduce the possibility of differential charging. Some of the suite of Cr(III) compounds chosen for study produced Cr 2p spectra containing fine structure that could be identified with multiplet splitting. The splitting patterns produced were similar for all trivalent binary and ternary oxides and sulphides whose patterns closely reproduced the splitting predicted for the Cr(III) free ion by Gupta and Sen. The fine structure observed for compounds such as chromium (III) chloride had a distinctly different pattern. A number of other chromium (III) compounds were studied that did not exhibit the fine structure described above; nonetheless, well-defined line shapes and reproducible peak centroids were obtained by fitting protocols. The use of such information to determine surface chemistry on chromated steels is described, based on the spectral knowledge of chromium (III) oxides and hydroxides and the chromium (VI) oxide systems. Copyright © 2004 John Wiley & Sons, Ltd.

KEYWORDS: XPS; Cr; chromium compounds

INTRODUCTION

X-ray photoelectron spectroscopy is widely used for studies of surface chemistry because it provides a range of useful information depths, reasonable quantitation and chemically specific information for each element detected, through the chemical shift. Despite successes in distinguishing some chemical differences for specific systems, progress towards a comprehensive knowledge base of chemical species for most elements has been slowing down. Chemical shifts originally were felt to reflect the partial charge density on a particular atomic site, but 'final state' effects during photoemission have been found to contribute to many systems. Also, peak shapes associated with most non-metallic systems studied have been broad and poorly defined due to surface charge-induced broadening and shifting. Moreover, some of the model compounds used in past investigations may have been contaminated as the result of surface reactivity with water vapour and oxygen. Finally, the bandpass of existing excitation photon sources has been proved to limit the ultimate resolution of the photoelectron spectra produced, thus affecting spectral definition—in some cases, severely.

There are several reasons why the time is appropriate for a major campaign to explore anew the effects of chemical bonding on XPS spectra. First, from a technological standpoint, a recently developed electron spectrometer, the Kratos Axis Ultra, has demonstrated unparalleled control of surface charging along with state-of-the-art spectral

resolution, detection sensitivity and bandpass of its x-ray exciting source. Second, final-state effects such as multiplet splitting and shake-up can give rise to additional fine structure in the core line photoelectron spectra—structures are finally becoming recognized as measurements that could be as useful as the chemical shift in detecting differences in surface chemistry. Our work on iron and nickel oxides in the 1970s was one of the first efforts to use multiplet splitting in this manner.^{1,2} In the past these structures have been difficult to analyse, but new instrumental developments have changed this. Core line spectra of exceptionally high signal-to-noise ratio and much improved resolution can be acquired in minutes rather than hours, as was the case previously. Access to an intense synchrotron exciting source promises even better definition in the future. Using an available Kratos system, we have begun to explore the detailed XPS spectra of first-row transition elements, beginning with those of iron and chromium. Of interest here are multiplet splitting and shake-up core line spectral changes as a result of: changes in formal oxidation state of the metal ion; effects of crystal field geometry about the metal ion on such structures; and effects of charge transfer from back bonding. Improved definition of chemical shifts and Auger parameters is also of interest. Finally, preparative protocols for the analysis of chemical compounds by XPS have improved: compounds can be treated to avoid or remove water and other surface contaminants by their introduction under inert gas cover and/or gently heating them *in vacuo*. No spectrum should be deemed acceptable until the surface concentration of impurity elements or compounds is low, and the quantitative elemental composition of the compound

*Correspondence to: M. C. Biesinger, Surface Science Western, Room G1, Western Science Centre, University of Western Ontario, London, Ontario, N6A 5B7, Canada. E-mail: biesingr@uwo.ca

under study corresponds to that expected from chemical stoichiometry.

This paper documents our detailed studies of a number of chromium compounds, mostly with a Cr(III) oxidation state. Our initial interest with these was to define spectral changes to Cr(III) in a Cr₂O₃ corundum-like structure, because divalent nickel and iron surround each chromium tetrahedrally in the ternary chromites. Recently, high-resolution Cr 2p spectra of Cr₂O₃ have been published by two groups^{3,4} that point out the existence of a multiplet structure previously identified by our group. It is important that such information be promulgated because there have been many past attempts to ascribe such structures as arising from multiple chemical states. New spectral information on the chromites is of practical interest as well because such structures could figure prominently in the surface oxides present on many nickel alloys and stainless steels. Beyond the spectra for these oxides, the study of Cr(III) halides allows the effects of the ligand field on the Cr(III) ion to be studied in detail; such spectra, along with those of the hydroxide, phosphate and sulphide, are presented below along with an initial attempt to analyse the changes to multiplet splitting in the context of the free ion splittings calculated by Gupta and Sen (GS).^{5,6}

In addition to the fundamental aspects of the spectra, this paper addresses some of the issues to be faced in identifying one chromium species in the presence of others. One of the most practical examples faced by this laboratory has been the detection of chromate species in thin films of chromium oxides mostly in the Cr(III) state. Based on the spectral information from this study, we propose an analysis protocol for chromium oxide specimens.

EXPERIMENTAL

The XPS Instrument

The XPS analyses were carried out with a Kratos Axis Ultra spectrometer using a monochromatic Al K α source (15 mA, 14 kV). The instrument work function was calibrated to give a binding energy (BE) of 83.96 eV for the Au 4f_{7/2} line for metallic gold and the spectrometer dispersion was adjusted to give a BE of 932.62 eV for the Cu 2p_{3/2} line of metallic copper. This instrument is equipped with a stage capable of being heated to 600 °C and cooled to approximately -120 °C. The Kratos charge neutralizer system was used on all specimens except the metal, with the following settings: filament current 1.6 A, charge balance 2.4 V, filament bias 1.0 V and magnetic lens trim coil 0.375 A. High-resolution spectra of all major lines were taken using a 10 eV and/or 20 eV pass energy and an analysis area of ~300 × 700 μm. An argon atmosphere glove-box attached to one of the two XPS reaction chambers allowed for introduction of air-/water-sensitive samples. Mineral samples were fractured in a vacuum using an attached knife-edged cleaver. Powder samples were mounted in a 1.5 mm diameter, 1.5 mm deep hole in a stainless steel or copper stub.

Spectra were analysed using CasaXPS software,⁷ version 2.2.19. In some cases narrowing of spectral resolution was carried out with maximum entropy method (MEM) software

developed in this laboratory⁸ using a resolution function with a width of 0.35 eV for a pass energy setting of 10 eV.

Preparation of samples

Chromium metal was obtained in 99.99% purity from Alfa Aesar (Ward Hill, MA) and sputtered with an argon ion beam to remove all oxide contamination before its analysis.

The minerals eskolaite (Cr₂O₃), chromite (FeCr₂O₄) and crocoite (PbCrO₄) were obtained from the Royal Ontario Museum (ROM) in chunk form capable of being cleaved in a vacuum. A separate sample of chromite was obtained from the Geological Survey of Canada. The oxide Cr₂O₃ was obtained as a pure synthetic material (Alfa Aesar) in a vacuum-cleavable chunk. Structures were confirmed by x-ray diffraction and their compositions by energy-dispersive x-ray (EDX) analysis using a Hitachi S4500 scanning electron microscope equipped with an EDAX light element detector. Samples were cleaved several times in an ultrahigh vacuum (UHV) within the instrument using a diamond knife-edge, as well as being introduced following air cleaving. The oxide NiCr₂O₄ (90% purity) was obtained from Alfa Aesar in powder form and was loaded into the spectrometer from the air. Most oxides were heated in a vacuum during the studies to determine if this caused any spectral changes.

The compounds CrF₃, CrCl₃, CrBr₃·6H₂O, Cr₂S₃, Cr₂(SO₄)₃·xH₂O and CrPO₄·4H₂O were obtained in powder form in >99% purity from Alfa Aesar. The fluoride and chloride were shipped under argon and transferred to the spectrometer in the glove-box, as was the Cr₂S₃. Both the trifluoride and trichloride were heated to >500 °C in a vacuum and the trifluoride to 1100 °C in argon in an attempt to induce a more well-resolved spectral structure, but with negative results. Chromium (III) hydroxide was prepared by precipitation from a 1.0 M chromium (III) chloride (CrCl₃·6H₂O) solution with 0.1 M aqueous ammonia.⁹ The precipitate was allowed to settle and the liquid decanted off. The precipitate was then re-suspended in fresh aqueous ammonia. This process was repeated three times, with the final product centrifuged and dried under a vacuum at room temperature. Using EDX spectroscopy, the product was found to be free of chlorine. An x-ray diffraction spectrum of the product gave a match for hydrated chromium (III) hydroxide (Cr(OH)₃·xH₂O). The XPS spectrum was recorded several times under a vacuum and following heating in a vacuum.

A record of the measured composition and spectral purity of each compound from the recorded XPS spectra is presented in Table 1. Of particular interest here are the elemental atomic ratios, which give the best indication that measured spectra are in fact those for the proper compound and not that of a structure that has been transformed by effects such as vacuum desiccation or x-ray degradation. Also, the absence of other possible impurities is important. All BEs were corrected for surface charging by correcting the C 1s line centroid (main peak, adventitious carbon or C–C, C–H) to a BE of 285.0 eV. It is recognized that the uncertainty on this is at least 0.2 eV because there is increasing evidence that the adventitious carbon signal is not constant on all surfaces.^{10,11}

Table 1. The XPS compositions (in at. %), primary anion/chromium ratios and preparation notes

Compound/treatment	Glove box	Vacuum fracture	Primary intensity ratio	Composition (at. %)								
				Cr	O	C	F	Cl	S	Other		
CrF ₃ (packed in argon, 1st analysis)	Y		F/Cr	19.5	5.2	18.5	56.5	0.4				
CrF ₃ (packed in argon, 2nd analysis)	Y		F/Cr	19.3	5.5	19.5	55.7					
CrF ₃ (heated in argon, 1100 °C, 1 h)			F/Cr	20.7	10.7	19.4	48.1					Na 1.1
CrCl ₃ (packed in argon)	Y		Cl/Cr	19.4	8.1	19.3		53.2				
CrCl ₃ (regular packing, 1st analysis)			Cl/Cr	25.0	3.5	1.8		69.7				
CrCl ₃ (regular packing, 2nd analysis)			Cl/Cr	21.3	3.4	8.9		66.4				
CrCl ₃ (regular packing, 3rd analysis)			Cl/Cr	20.8	3.0	13.7		62.5				
CrBr ₃ ·6H ₂ O			Br/Cr	7.0	20.4	45.6						Br 25.5 N 1.5
Cr ₂ S ₃	Y		S/Cr	11.1	25.3	41.6				22.1 ^a		
Cr ₂ (SO ₄) ₃ ·xH ₂ O			S/Cr	8.0	69.1	9.3				11.8		N 1.8
CrPO ₄ ·4H ₂ O			P/Cr	3.7	34.3	52.8				0.4		P 2.0 Na 2.0 N 0.6 Al 1.9
Cr(OH) ₃ (hydrated freshly made)			O/Cr	6.8	29.5	63.8						
Cr(OH) ₃ (hydrated 3 months old)			O/Cr	21.2	66.4	8.0		0.8				N 1.7 Ca 0.7 Mg 1.2
Cr(OH) ₃ (heated 2 h at 50 °C)			O/Cr	21.6	62.2	12.1		0.8				N 1.5 Ca 0.7 Mg 1.1
Cr(OH) ₃ (heated 18 h at 50 °C)			O/Cr	21.4	59.5	13.5		1.3				N 2.2 Ca 0.7 Mg 1.3
Cr(OH) ₃ (heated 50 °C, 18 h; 550 °C, 1 h)			O/Cr	26.7	51.4	16.7		0.7				N 2.2 Ca 1.1 Mg 1.2
Cr ₂ O ₃ (Fresh)		Y	O/Cr	28.4	50.1	11.6				1.0		Na 2.1 N 1.3 Ca 0.7 Mg 2.4 Si 2.5
Cr ₂ O ₃ (air-fractured)		Y	O/Cr	24.1	49.7	17.3						Na 4.4 Si 4.5
Cr ₂ O ₃ (old sample, heated 550 °C, 3 h)		Y	O/Cr	32.1	45.3	15.7				0.9		Na 2.4 Mg 0.8 Si 2.8
Eskolaite (Cr ₂ O ₃ , 1st analysis)		Y	O/Cr	24.1	61.7	10.0						Fe 2.3 Al 1.3 Ti 0.5
Eskolaite (Cr ₂ O ₃ , 2nd analysis)		Y	O/Cr	26.2	63.2	6.9						Fe 2.0 Al 1.3 Ti 0.4
Chromite (FeCr ₂ O ₄)		Y	O/Cr	18.0	57.9	3.1						Fe 4.9 Mg 11.0 Al 3.0 Si 2.2
Chromite (FeCr ₂ O ₄ , cooled)		Y	O/Cr	7.0	57.5	11.5						Fe 2.5 Mg 11.9 Al 2.7 Si 6.9
Chromite (FeCr ₂ O ₄ , air-fractured)			O/Cr	12.0	51.4	19.6						Fe 3.7 Mg 7.0 Al 2.4 Si 4.0
NiCr ₂ O ₄ (1st analysis)			O/Cr	25.8	52.1	7.2						Ni 11.1 Na 3.8
NiCr ₂ O ₄ (2nd analysis)			O/Cr	23.1	49.3	15.6						Ni 9.1 Na 2.9
Crocoite (PbCrO ₄ , Cr(VI))		Y	O/Cr	11.8	46.3	27.7						Pb 14.2

^a Some sulphate contamination.

RESULTS

Chromium oxides

The best representative high-resolution spectra for Cr_2O_3 cleaved in a vacuum are shown in Fig. 1. The Cr 2p spectrum in Fig. 1(a) shows a clearly structured shape with about the same peak separations as shown in two recent publications.^{3,4} For this particular compound, the five multiplet splitting peaks are fitted to the envelope with half-widths of ~ 0.9 eV and separations of 1.0, 0.8, 1.0 and 0.8 eV (see Tables 2 and 3).

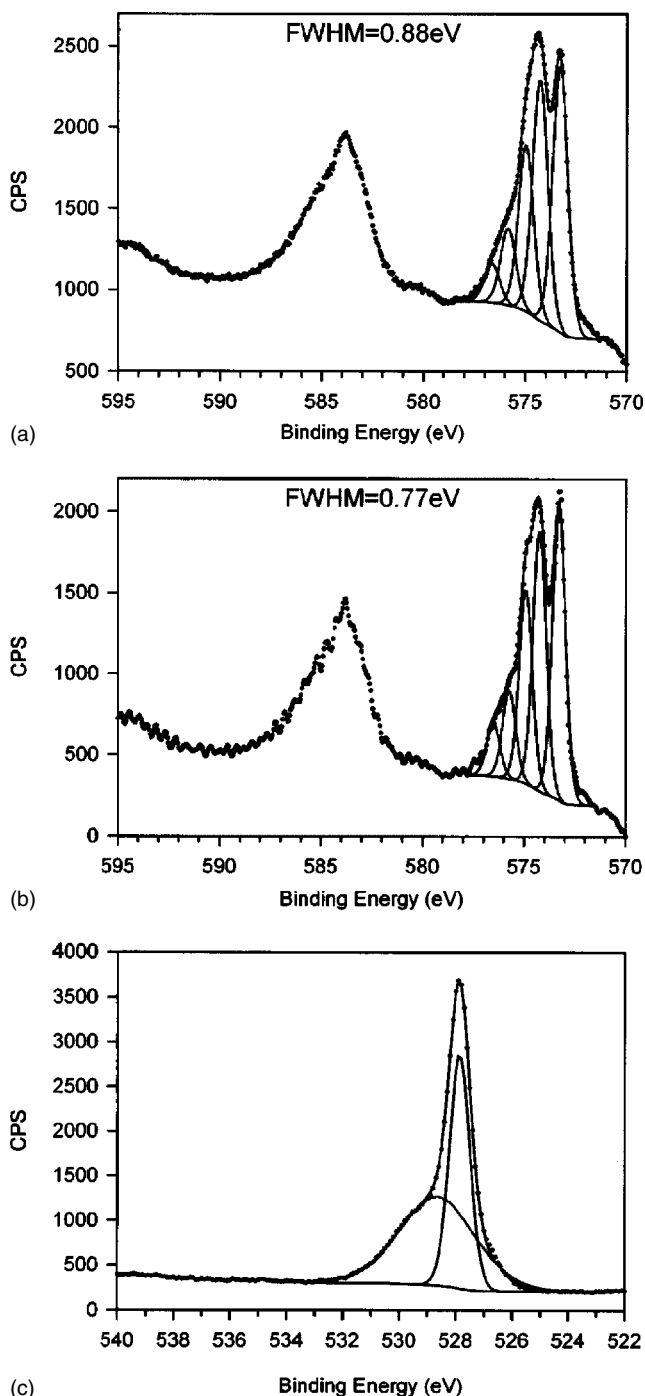


Figure 1. Spectra for vacuum-fractured Cr_2O_3 (Alfa Aesar): (a) Cr 2p; (b) Cr 2p after MEM treatment; (c) O 1s. All spectra except Fig. 14 are presented uncorrected for charging. Charge-corrected values are presented in the various tables.

Some improved detail is obtained through the use of the MEM filter and this is shown in Fig. 1(b) ($\text{FWHM} = 0.77$ eV). The relative intensities and splittings can be compared with the free ion multiplet splitting values calculated by Gupta and Sen^{5,6} using a simple Hartree–Fock model of the interaction (see Table 3); the agreement between splitting for the oxide and free ion is remarkable. Although such detailed analyses are instructive in cases where the compound studied does produce a clear splitting, as is the case here, it is also possible to produce a single peak definition of the peak that serves to compare weighted BEs for all Cr $2p_{3/2}$ spectra in this study—for both those with and without fine structure. Thus, Table 4 shows carbon-corrected single Gaussian–Lorentzian peak fits of the Cr $2p_{3/2}$ envelope. Figure 1(c) shows the O 1s spectrum for Cr_2O_3 fitted to show the component due to substitutional oxygen, as well as those oxygen species associated with interstitial and surface sites. Table 5 gives carbon-corrected O 1s BEs for the substitutional oxygen (530.3 ± 0.2 eV) as well as for the surface or near-surface species. The mineral eskolaite, essentially Cr_2O_3 , was also analysed after vacuum fracture and gave a similar shape, although not as well-resolved and with corrected BEs that were slightly higher than those of the pure compound.

Air cleaving of any of the available Cr_2O_3 specimens resulted in considerably broader Cr $2p_{3/2}$ and O 1s spectra, as shown in Fig. 2. The Cr $2p_{3/2}$ multiplet splitting structure was practically emasculated. After fitting this spectrum with a single peak, the carbon-corrected BE position of

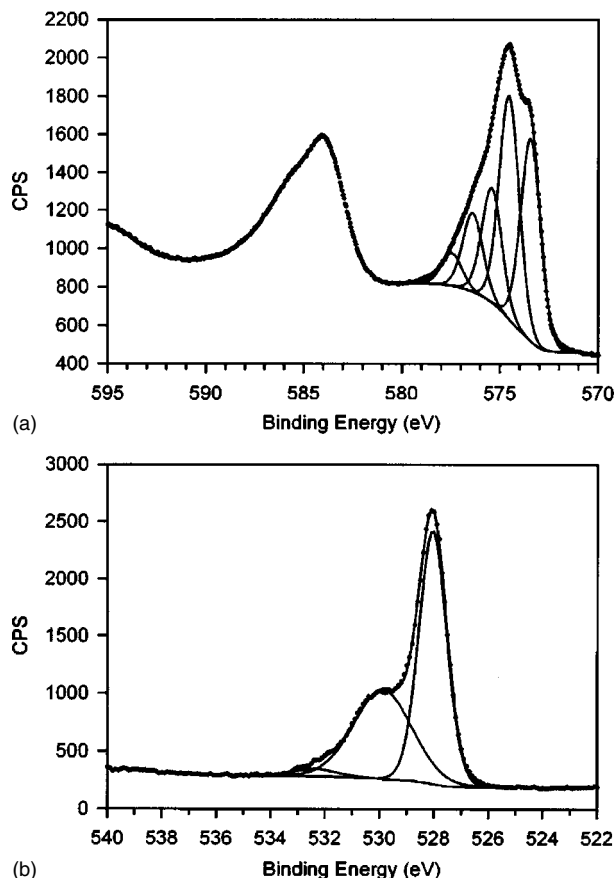


Figure 2. Spectra for air-fractured Cr_2O_3 (Alfa Aesar): (a) Cr 2p; (b) O 1s.

Table 2. Results from Cr 2p_{3/2} multiplet splitting fitted spectra, with all BEs corrected to C 1s at 285.0 eV

Compound/treatment	Pass energy	FWHM (multiplets)	Peak 1	%	Peak 2	%	Peak 3	%	Peak 4	%	Peak 5	%	Weighted av. of first two multiplets	Weighted av. of all multiplets	Single peak fits from Table 4
CrCl ₃ (packed in argon)	10	0.88	576.8	44.9	577.8	33.1	578.5	17.5	579.5	4.6			577.2	577.5	577.6
	20	0.95	577.0	45.8	578.0	32.6	578.7	17.4	579.7	4.3			577.4	577.7	577.4
CrCl ₃ (regular packing, 1st analysis)	10	0.78	577.3	47.9	578.3	32.0	579.0	16.1	580.1	4.0			577.7	578.0	577.9
	20	0.83	577.4	48.1	578.4	33.3	579.1	15.3	580.1	3.3			577.8	578.1	577.9
CrCl ₃ (regular packing, 2nd analysis)	20	0.88	576.7	41.5	577.6	31.1	578.3	22.4	579.3	5.0			577.1	577.5	577.4
	10	0.92	577.4	46.9	578.4	32.0	579.1	17.4	580.2	3.7			577.8	578.1	578.0
Cr ₂ S ₃	10	0.91	574.2	33.3	575.1	27.3	575.8	14.4	576.6	3.1			574.6	574.9	574.8 ^a
	10	0.88	575.8	33.8	576.7	30.5	577.4	21.1	578.3	9.7	579.1	4.9	576.2	576.8	576.7
Cr ₂ O ₃ (fresh, vacuum-fractured)	10	0.94	575.7	34.0	576.7	31.8	577.5	20.0	578.4	9.5	579.2	4.7	576.2	576.8	576.6
	20	1.20	575.6	31.1	576.7	34.4	577.6	17.5	578.6	12.0	579.6	5.0	576.2	576.9	576.7
Cr ₂ O ₃ (air-fractured)	20	1.31	575.7	30.2	576.9	36.2	577.9	18.8	578.9	11.4	580.1	3.4	576.3	577.0	576.8
	10	0.95	576.5	30.2	577.5	26.8	578.2	16.6	579.2	7.4	580	3.0	577.0	577.5	577.2 ^b
Cr ₂ O ₃ (old sample, heated 550 °C, 3 h)	20	0.98	576.5	28.9	577.5	26.1	578.2	15.6	579.1	6.7	579.9	3.0	577.0	577.5	577.1 ^c
	10	1.04	576.0	36.6	577.0	35.5	577.8	19.9	578.8	8.0			576.5	576.9	576.8
Eskolaite (Cr ₂ O ₃ , 1st analysis)	20	1.12	576.1	37.6	577.1	37.3	577.9	17.7	579.0	7.4			576.6	577.0	576.9
	10	1.10	576.1	36.8	577.2	38.0	578.0	17.9	579.1	7.4			576.6	577.1	576.9
Eskolaite (Cr ₂ O ₃ , 2nd analysis)	10	1.03	576.1	43.6	577.1	36.8	577.9	13.3	579.0	6.3			576.5	576.9	576.7
	20	1.10	576.1	41.9	577.2	41.9	578.1	11.3	579.2	4.9			576.6	576.9	576.7
Chromite (FeCr ₂ O ₄ , cooled)	10	1.46	576.3	38.5	577.4	39.0	578.3	15.0	579.3	7.5			576.9	577.3	577.1 ^d
	20	1.20	576.0	40.1	577.1	37.9	578.0	14.4	579.0	7.5			576.6	577.0	576.8
Chromite (FeCr ₂ O ₄ , air-fractured)	10	1.20	575.9	42.3	577.0	37.8	577.8	13.4	578.9	6.6			576.4	576.7	576.6
	20	1.28	576.2	43.9	577.3	39.0	578.2	11.0	579.2	6.0			576.7	577.0	576.8
NiCr ₂ O ₄ (1st analysis)	10	1.01	575.5	35.1	576.5	34.0	577.3	17.4	578.4	8.6	579.6	5.0	576.0	576.6	576.3
	10	1.17	575.3	34.1	576.3	34.7	577.2	19.2	578.2	8.9	579.2	3.0	575.8	576.4	576.2

^a Peak at 577.1 eV, 13.7%, FWHM 2.0 eV (Cr oxides and hydroxide species); peak at 578.5 eV, 8.3%, FWHM 2.0 eV (Cr₂(SO₄)₃).^b Peak at 575.2 eV, 16.1%, FWHM 2.25 eV.^c Peak at 575.2 eV, 19.7%, FWHM 2.37 eV.^d Broadened?

Table 3. Averages of BE values, peak separations and weightings for multiplet split spectra

Compound/no.	Peak 1 (eV)	%	Peak 2 (eV)	Δ Peak 1/ Peak 2	%	Peak 3 (eV)	Δ Peak 2/ Peak 3	%	Peak 4 (eV)	Δ Peak 3/ Peak 4	%	Peak 5 (eV)	Δ Peak 4/ Peak 5	%	Av. of weighted av. of first two multiplets	Av. of weighted av. of all multiplets	Av. of single peak fits from Table 4
CrCl ₃ —av. of 6	577.1	46	578.1	0.99	32	578.8	0.71	18	579.8	1.03	4	577.5	577.8	577.7			
Cr ₂ S ₃ —single	574.2	33	575.1	0.95	27	575.8	0.67	14	576.6	0.81	3	574.6	574.9	574.8			
Cr ₂ O ₃ —av. of 5	575.9	36	576.9	1.01	35	577.7	0.78	19	578.7	1.00	8	576.4	576.9	576.8			
Chromite—av. of 4	576.1	41	577.2	1.09	39	578.1	0.88	13	579.1	1.04	7	576.7	577.0	576.8			
NiCr ₂ O ₄ —av. of 2	575.4	35	576.4	1.02	34	577.2	0.81	18	578.3	1.05	9	575.9	576.5	576.2			
Cr(III) free ion (Gupta and Sen) ^{6a}		47		1.09	41		0.9	7		2.34	4	NA	NA	NA			

^a Peak fit of first five components from a digitized reproduction of the graph from the original paper.⁶

Table 4. Results from Cr 2p_{3/2} single peak-fitted spectra (Cr 2p BEs are corrected to C 1s at 285.0 eV; C 1s BEs are uncorrected)

Compound/treatment	Pass energy	C 1s uncorrected	Correction	Cr 2p	FWHM
CrF ₃ (packed in argon, 1st analysis)	10	282.43	2.57	580.1	2.74
CrF ₃ (packed in argon, 2nd analysis)	10	282.58	2.42	580.1	2.72
CrF ₃ (heated in argon, 1100 °C, 1 h)	10	282.62	2.38	580.0	2.76
CrCl ₃ (packed in argon)	10	282.66	2.34	577.6	2.20
	20	282.68	2.32	577.4	2.17
CrCl ₃ (regular packing, 1st analysis)	10	282.73	2.27	577.9	2.11
	20	282.73	2.27	577.9	2.11
CrCl ₃ (regular packing, 2nd analysis)	20	282.30	2.70	577.4	2.14
CrCl ₃ (regular packing, 3rd analysis)	10	282.34	2.66	578.0	2.13
CrBr ₃ ·6H ₂ O	20	283.69	1.31	576.9	2.80
Cr ₂ S ₃	10	282.81	2.19	574.8	1.98
Cr ₂ (SO ₄) ₃ ·xH ₂ O	10	283.68	1.32	578.5	2.62
CrPO ₄ ·4H ₂ O	10	282.36	2.64	577.9	2.29
Cr(OH) ₃ (hydrated) (freshly made)	10	282.19	2.81	577.3	2.51
Cr(OH) ₃ (hydrated 3 months old)	10	283.09	1.91	577.5	2.85
Cr(OH) ₃ (heated 2 h at 50 °C)	10	283.19	1.81	577.6	3.04
Cr(OH) ₃ (heated 18 h at 50 °C)	10	283.38	1.62	577.5	3.17
Cr(OH) ₃ (heated 50 °C, 18 h; 550 °C, 1 h)	10	283.67	1.33	576.7	3.17
Cr ₂ O ₃ (fresh, vacuum-fractured)	10	282.54	2.46	576.7	2.53
	20	282.68	2.32	576.6	2.55
Cr ₂ O ₃ (air-fractured)	10	282.82	2.18	576.7	2.91
	20	282.87	2.13	576.8	3.00
Cr ₂ O ₃ (old sample, heated 550 °C, 3 h)	10	284.87	0.13	577.2	2.80
	20	284.85	0.15	577.1	2.89
Eskolaite (Cr ₂ O ₃ , 1st analysis)	10	282.84	2.16	576.8	2.36
	20	282.84	2.16	576.9	2.39
Eskolaite (Cr ₂ O ₃ , 2nd analysis)	10	282.61	2.39	576.9	2.38
Chromite (FeCr ₂ O ₄)	10	283.31	1.69	576.7	2.28
	20	283.31	1.69	576.7	2.31
Chromite (FeCr ₂ O ₄ , cooled)	10	282.29	2.71	577.1	2.61
	20	282.33	2.67	576.8	2.53
Chromite (FeCr ₂ O ₄ , air-fractured)	10	282.29	2.71	576.6	2.42
	20	282.30	2.70	576.8	2.42
NiCr ₂ O ₄ (1st analysis)	10	283.25	1.75	576.3	2.49
NiCr ₂ O ₄ (2nd analysis)	10	283.64	1.36	576.2	2.54
Crocoite (PbCrO ₄ , Cr(VI))	10	283.91	1.09	578.9	0.85
	20	283.91	1.09	579.1	0.91
Cr (metal, sputter-cleaned)	10	a	a	574.2	0.85

^a Referenced to Au 4f_{7/2} at 83.95 eV.

the single peak fit (Table 4) is virtually identical to that for the vacuum-cleaved specimen measured by the same protocol (576.7 ± 0.1 eV). The fitted O 1s spectrum is shown in Fig. 2(b), and the corrected BE (Table 5) is the same as for the vacuum-cleaved specimen. The air-cleaved specimen was heated in a vacuum at 550 °C for 3 h. Its Cr 2p spectrum (Fig. 3) was transformed to produce a clean multiplet structure comparable to the vacuum-cleaved specimen. The corrected BEs (Table 2) were not consistent with those of other samples of the oxide, probably because of poor electrical contact of the heated oxide with the adventitious carbon used for charge correction procedures.

Spectra obtained for Cr(OH)₃ immediately after preparation are shown in Fig. 4. The Cr 2p_{3/2} line (Fig. 4(a)) has a width that is quite similar to that for air-cleaved Cr₂O₃, but

without the slight inflections on high and low BE sides of the envelope that appear to be characteristic for the oxide; thus, no evidence of individual multiplet components is seen. The carbon-corrected value (Table 4) for the single peak fitting (577.3 eV) is 0.6 eV above that for the oxide. In the O 1s spectrum (Fig. 4(b)), the hydroxyl peak is assigned to the most intense peak (531.8 eV); the peak at the lower BE results from a Cr₂O₃ impurity; the peak at the higher BE is assigned to water of hydration. The hydroxide was re-examined as a function of time in the vacuum, as well as following gentle heating under a vacuum; such treatment caused a broadening of the Cr 2p_{3/2} line and an upward drift in the corrected BE—probably the result of poor charge equilibrium within the specimen and with the calibrating carbon line (Table 4).

Table 5. Results from O 1s spectra (BEs corrected to C 1s at 285.0 eV)

Compound/treatment	Pass energy	Peak 1			Peak 2			Peak 3		
		O 1s	FWHM	%	O 1s	FWHM	%	O 1s	FWHM	%
Cr(OH) ₃ (hydrated) (freshly made)	10	530.1	1.26	7.8	531.8	1.70	80.7	533.6	1.42	11.4
Cr(OH) ₃ (hydrated 3 months old)	10	530.0	1.66	9.9	531.6	1.71	61.6	532.8	2.87	28.5
Cr(OH) ₃ (heated 2 h at 50 °C)	10	530.0	1.43	8.0	531.7	1.87	59.6	533.2	3.42	32.5
Cr(OH) ₃ (heated 18 h at 50 °C)	10	529.9	1.49	7.3	531.6	1.98	60.7	533.4	3.42	32.0
Cr(OH) ₃ (heated 50 °C, 18 h; 550 °C, 1 h)	10	529.9	1.77	38.9	531.4	2.14	43.3	533.2	3.25	17.7
Cr ₂ O ₃ (fresh, vacuum-fractured)	10	530.3	0.84	41.3	531.1	3.15	58.7			
	20	530.3	0.89	42.9	531.1	3.08	57.1			
Cr ₂ O ₃ (air-fractured)	10	530.2	1.19	56.4	532.1	2.50	41.1	534.5	1.81	2.6
	20	530.4	1.32	56.5	532.1	2.33	40.5	534.3	1.54	3.0
Cr ₂ O ₃ (old sample, heated 550 °C, 3 h)	10				531.1	1.15	89.0	533.3	2.31	11.0 ^a
	20				531.2	1.17	92.3	533.3	1.74	7.7 ^a
Eskolaite (Cr ₂ O ₃ , 1st analysis)	20	530.0	1.04	23.6	531.2	2.07	76.4			
Eskolaite (Cr ₂ O ₃ , 2nd analysis)	10	530.0	1.02	23.7	531.3	2.08	76.3			
Chromite (FeCr ₂ O ₄)	20	530.4	1.00	67.6	531.5	3.13	32.4			
Chromite (FeCr ₂ O ₄ , cooled)	10	530.2	0.93	18.2	531.6	2.29	81.8			
	20	530.3	0.98	20.3	531.8	2.33	79.8			
Chromite (FeCr ₂ O ₄ , air-fractured)	10	530.2	0.95	49.7	531.5	2.30	50.3			
	20	530.6	0.98	43.2	531.5	2.30	56.8			
NiCr ₂ O ₄ (1st analysis)	10	530.2	0.91	66.1	531.0	2.09	33.9			
NiCr ₂ O ₄ (2nd analysis)	10	530.2	0.96	62.4	531.1	2.22	37.6			
Crocoite (PbCrO ₄ , Cr(VI))	20	530.1	1.01	81.6	531.0	2.03	18.4			

^a Carbon 1s peak shows very little or no charging.

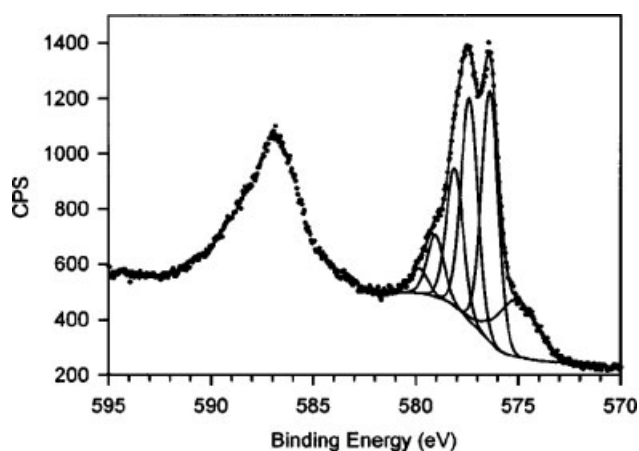


Figure 3. Chromium 2p spectrum from aged Cr₂O₃ (Alfa Aesar) after heating in a vacuum to 550 °C for 3 h.

Spectra for the ternary spinel oxides FeCr₂O₄ and NiCr₂O₄ are shown in Figs 5 and 6, respectively. The FeCr₂O₄ (chromite) spectra were obtained following cleaving of specimens in air and in a vacuum; both produced essentially identical spectra. These were well-resolved Cr 2p spectra with obvious multiplet structure (Fig. 5(a)) whose splitting and intensities are analysed in Table 3. The MEM treatment resulted in slightly narrower spectral linewidths (Fig. 5(b)). In comparison to the structure observed for Cr₂O₃, the splitting of the clearest first two components has increased by ~10%. Another subtle change is in the area ratio (peak 1/peak 2) of the first two Cr 2p_{3/2} components for chromite, which is 1.2 compared with 1.1 for Cr₂O₃ (from the 10 eV

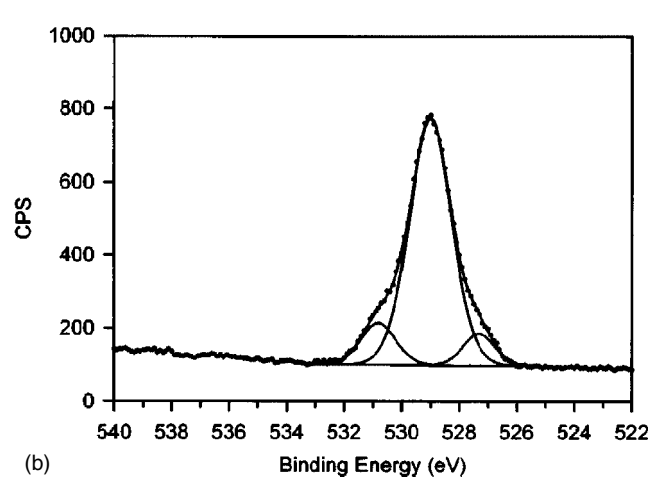
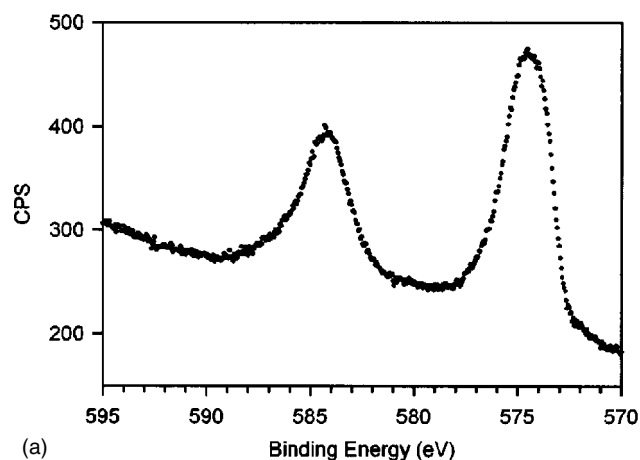


Figure 4. Spectra for freshly made Cr(OH)₃·xH₂O: (a) Cr 2p; (b) O 1s.

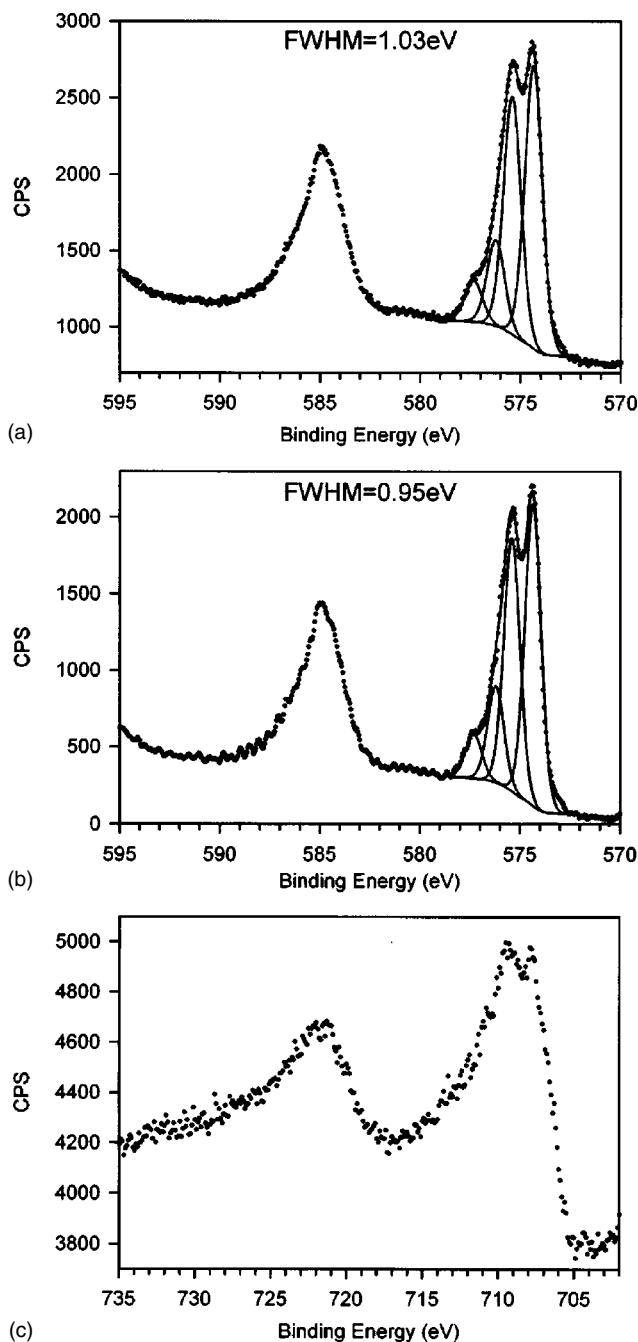


Figure 5. Spectra for vacuum-fractured chromite (FeCr_2O_4): (a) Cr 2p; (b) Cr 2p after MEM treatment; (c) Fe 2p.

pass energy spectra for both). The corrected BEs and relative intensities of the component peaks (Table 2) are virtually identical to those for Cr_2O_3 , with one important exception: the fifth spectral component observed for Cr_2O_3 at a BE of 579.1 eV is completely missing in the chromite spectrum. The Fe 2p spectrum (Fig. 5(c)) has a multiplet shape that is typical for ferrous iron, as observed in other studies under way in this laboratory.¹² The NiCr_2O_4 has a Cr 2p_{3/2} spectrum with a corrected centroid BE of 576.3 eV, which is ~0.4 eV below that for Cr_2O_3 . Aside from this, the multiplet structure is identical to that for Cr_2O_3 (Table 2), with the exception that the BE of the fifth multiplet component is set out a further 0.8 eV from the other components; this fifth

component (or absence of it) may be one of the most useful indicators in distinguishing Cr_2O_3 , FeCr_2O_4 and NiCr_2O_4 . The Ni 2p spectrum (Fig. 6(b)) for the nickel chromite differs substantially from that observed for NiO; detailed analysis will be carried out in a later publication. The O 1s spectrum for both of these ternary oxides (Table 5) shows a narrow peak (FWHM < 1 eV) for substitutional oxygen with the same BE position as for Cr_2O_3 within experimental error.

The spectra for vacuum-cleaved crocoite (PbCrO_4) are shown in Fig. 7; this Cr(VI) oxide is diamagnetic and therefore no multiplet splitting was expected; the sharp Cr 2p_{3/2} singlet (Fig. 7) confirms this. The measured linewidth of 0.85 eV is about the same for the narrowest multiplet components. The additional weak structure is ascribed to Cr_2O_3 and CrO_3 impurities.

Other chromium compounds

Spectra for the chromium (III) halides CrF_3 , CrCl_3 and $\text{CrBr}_3 \cdot 6\text{H}_2\text{O}$ are shown in Figs 8–10, and include spectra of the important counter-ions; in addition, BEs for these species are reported in Table 6. The fluoride and bromide spectra are broad and show no resolved multiplet splitting structure, even after heating or introduction under a vacuum. The corrected BEs (580.1 eV for CrF_3 and 576.9 eV for CrBr_3 ; Table 4) resulting from single peak fitting of these structures are clearly defined and well-separated, even though no fine

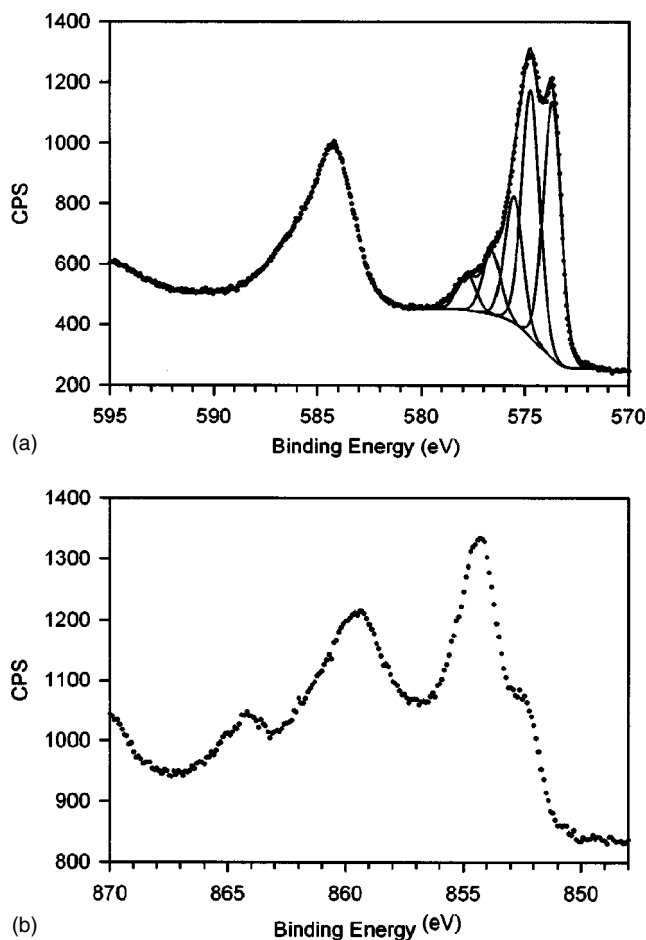


Figure 6. Spectra for nickel chromite (NiCr_2O_4): (a) Cr 2p; (b) Ni 2p.

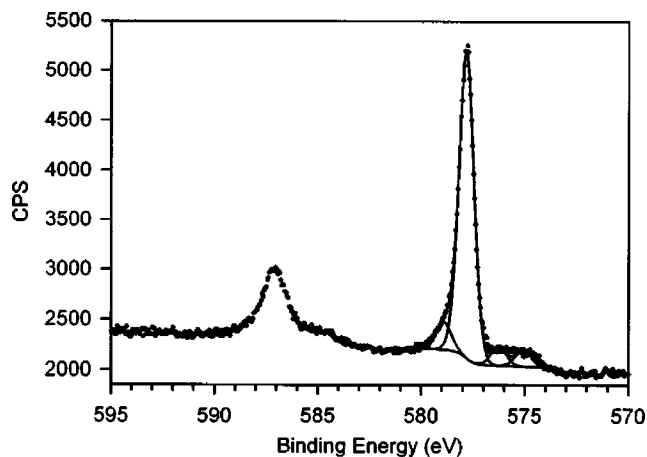
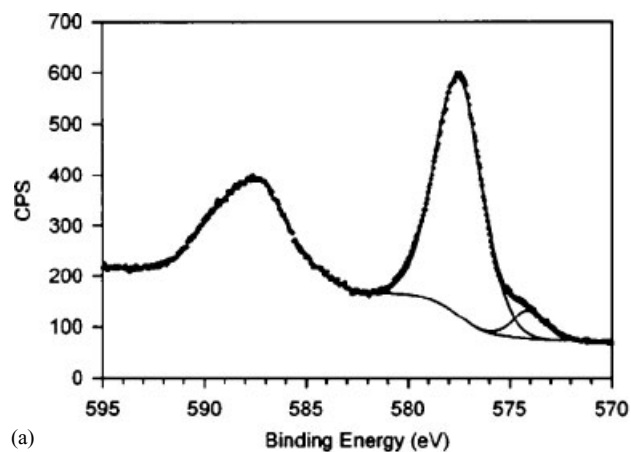
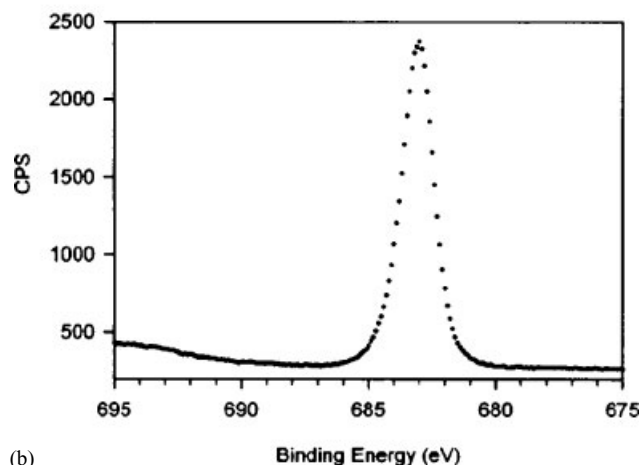


Figure 7. Chromium 2p spectrum for crocoite (PbCrO_4), a chromium (VI) compound.



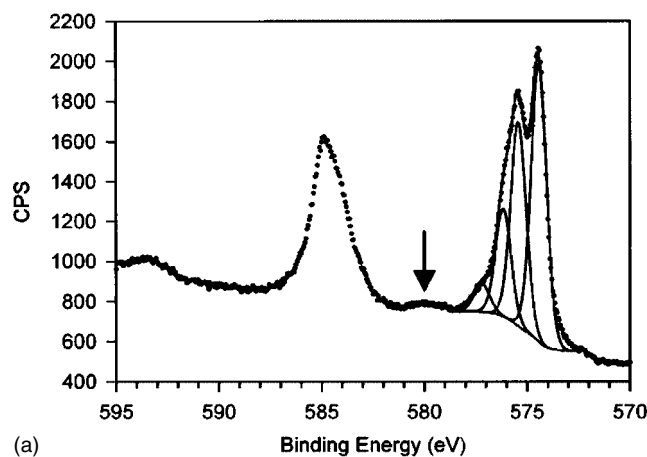
(a)



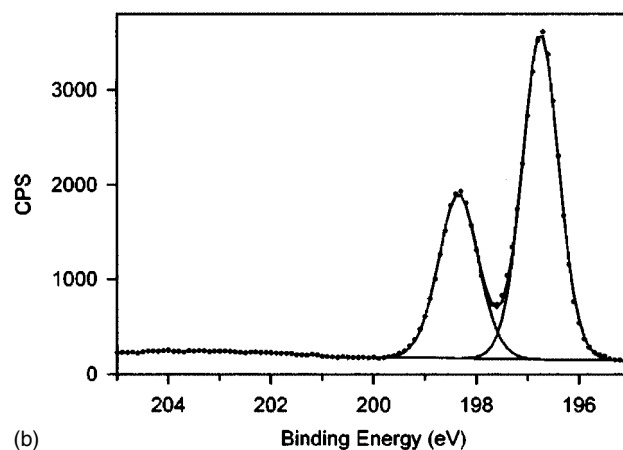
(b)

Figure 8. Spectra for CrF_3 : (a) Cr 2p; (b) F 1s.

multiplet splitting structure is apparent. By contrast, for the trichloride the multiplet structure is clearly revealed. Four multiplet components are well-defined (Fig. 9(a) and Table 2) with component splittings of 1.0, 0.7 and 1.0 eV (Table 3); the component peak intensity ratio (peak 1/peak 2) is ~ 1.5 compared with 1.1 for the Cr_2O_3 spectrum. A separate weak peak ~ 5.0 eV above the single peak centroid (see arrow in Fig. 9) is assigned to a shake-up process. The carbon-corrected single peak BE for the trichloride



(a)

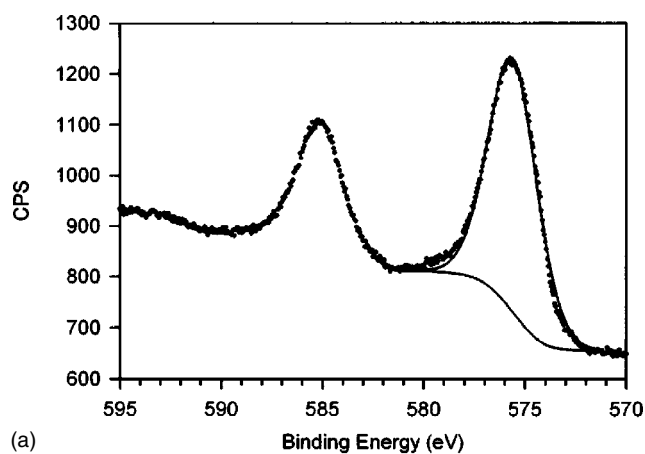


(b)

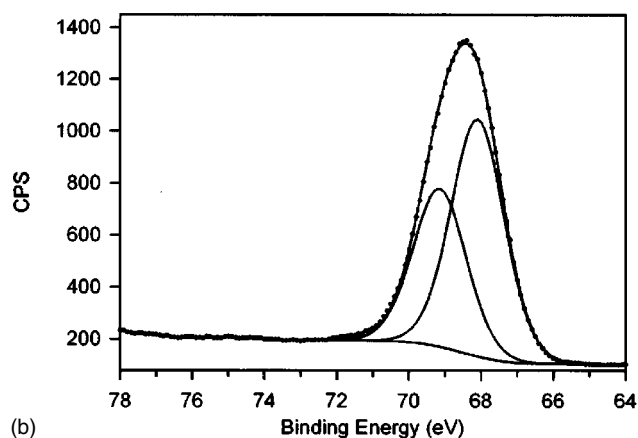
Figure 9. Spectra for CrCl_3 : (a) Cr 2p, where the arrow indicates the position of the shake-up peak; (b) Cl 2p.

(577.7 ± 0.2 eV) has a higher uncertainty (Table 4) because of inconsistent charge equilibrium between the sample and the adventitious carbon. This variability is also seen in the Cl 2p BEs given in Table 6. Spectra for Cr_2S_3 are also well-resolved (Fig. 11(a)) with component splittings of 0.95, 0.7 and 0.8 eV, which is $\sim 10\%$ smaller than the splitting for Cr_2O_3 . The S 2p spectrum (Fig. 11(b)) shows the presence of a narrow sulphide peak, as well as near-surface defects and a surface sulphate impurity; this latter is also observed in the Cr $2p_{3/2}$ spectrum as a high BE shoulder resulting from chromium sulphate, the identity and position of which is confirmed by the spectra for $\text{Cr}_2(\text{SO}_4)_3 \cdot x\text{H}_2\text{O}$ shown in Fig. 12. A spectrum of $\text{CrPO}_4 \cdot x\text{H}_2\text{O}$ is presented in Fig. 13. Both $\text{CrPO}_4 \cdot x\text{H}_2\text{O}$ and $\text{Cr}_2(\text{SO}_4)_3 \cdot x\text{H}_2\text{O}$ have broad Cr $2p_{3/2}$ lines that mask any evidence of multiplet components.

An attempt was made to measure the modified Auger parameter for each of the compounds studied. Unfortunately, the Cr $L_3M_{2,3}M_{2,3}$ Auger line is relatively weak, complex and close in energy to that for the OKLL line. Thus, measurement of the parameter was not found to be as reproducible as the corrected BEs for most of the chromium compounds. Furthermore, the Auger parameter shifts measured were generally, in addition to being less precise, smaller than the equivalent BE shifts.

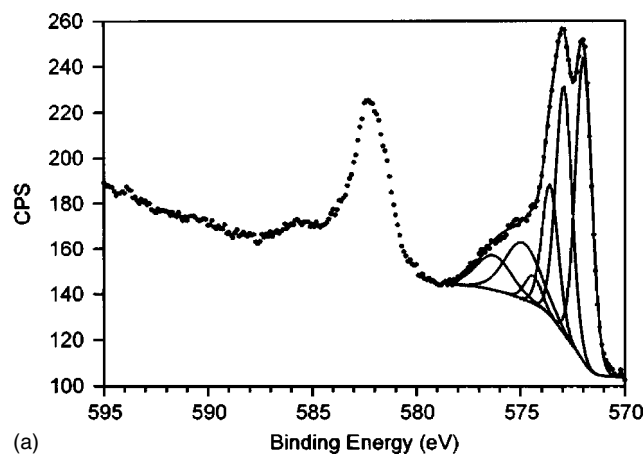


(a)

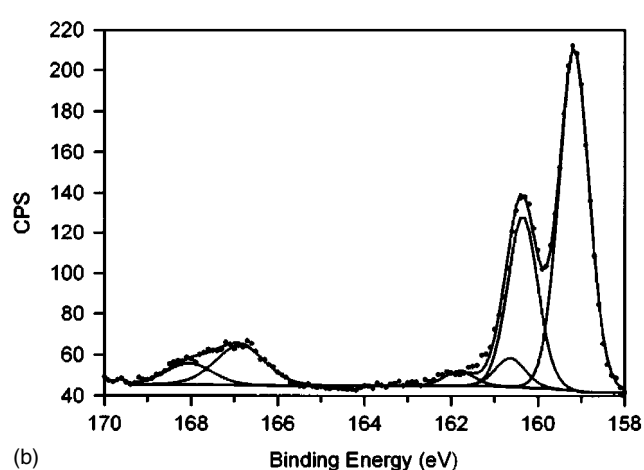


(b)

Figure 10. Spectra for $\text{CrBr}_3 \cdot 6\text{H}_2\text{O}$: (a) Cr 2p; (b) Br 3d.



(a)



(b)

Figure 11. Spectra for Cr_2S_3 : (a) Cr 2p; (b) S 2p.

DISCUSSION

This paper has shown that a number of chromium (III) compounds have inherent photoelectron line widths of 0.8–0.9 eV in half-width; such widths are comparable to those found for chromium metal and for a Cr(VI) oxide. This was achieved, in part, by the improved control of differential charging in this particular spectrometer, as well as by the narrow spectrometer resolution function. However,

there are clearly some additional effects that cause broader linewidths for some compounds than others. In the case of air-fractured Cr_2O_3 , thermal annealing led to a much better resolved spectrum, but such treatment had no effect for other compounds. Even for those compounds producing well-resolved spectral structure, a small step or 'pre-peak'¹² is frequently found to the low BE side of the envelope.

Table 6. Binding energy values (in eV) for chromium (III) compound anions, corrected to C 1s at 285.0 eV

Compound/treatment	Pass energy	F 1s		Cl 2p _{3/2}		Br 3d _{5/2}		S 2p _{3/2}		P 2p	
		F 1s	FWHM	Cl 2p _{3/2}	FWHM	Br 3d _{5/2}	FWHM	S 2p _{3/2}	FWHM	P 2p	FWHM
CrF ₃ (packed in argon, 1st analysis)	10	685.7	1.55								
CrF ₃ (packed in argon, 2nd analysis)	10	685.6	1.44								
CrF ₃ (heated in argon, 1100 °C, 1 h)	10	685.8	1.50								
CrCl ₃ (packed in argon)	10			199.1	0.83						
	20			199.7	0.89						
CrCl ₃ (regular packing, 1st analysis)	20			199.7	0.83						
CrCl ₃ (regular packing, 2nd analysis)	20			199.3	0.97						
CrCl ₃ (regular packing, 3rd analysis)	10			199.8	0.91						
CrBr ₃ ·6H ₂ O	20					69.4 ^a	1.73				
Cr ₂ S ₃	10							161.4 ^b	0.81		
Cr ₂ (SO ₄) ₃ ·xH ₂ O	10							169.5	1.50		
CrPO ₄ ·4H ₂ O	10									133.7	1.63

^a Broad Br peaks, spin orbit splitting not evident, fitted spectrum.

^b Small peak at 162.8 eV; a small amount of sulphate at 169.1 eV is also present.

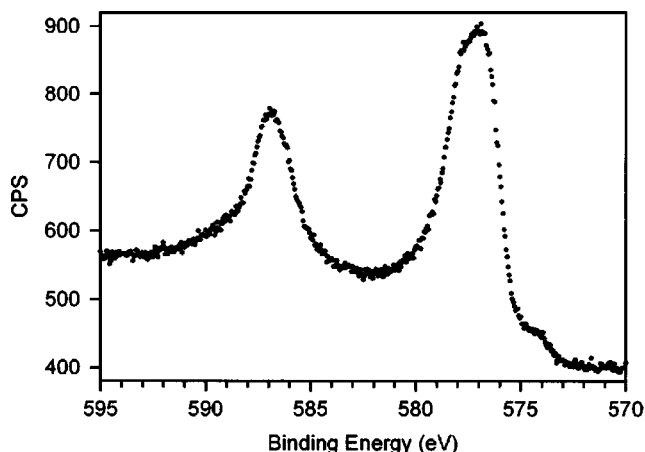


Figure 12. Chromium 2p spectrum for $\text{Cr}_2(\text{SO}_4)_3 \cdot x\text{H}_2\text{O}$.

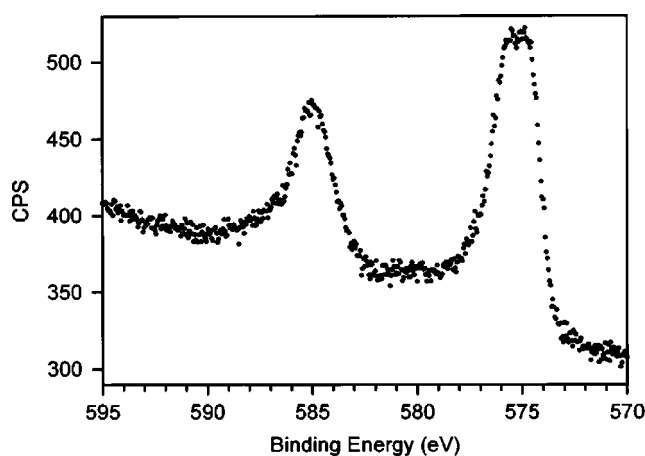


Figure 13. Chromium 2p spectrum for $\text{CrPO}_4 \cdot 4\text{H}_2\text{O}$.

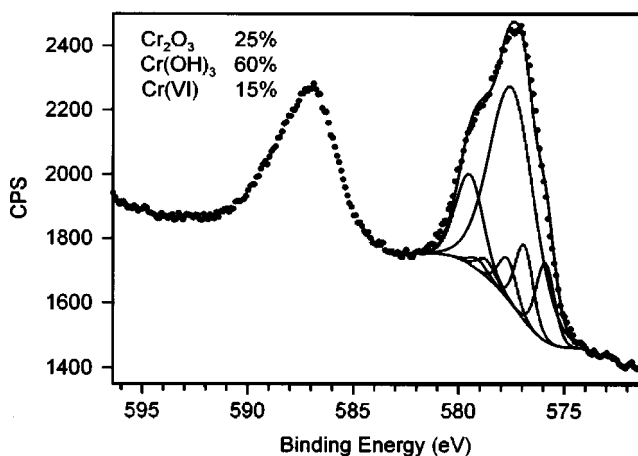
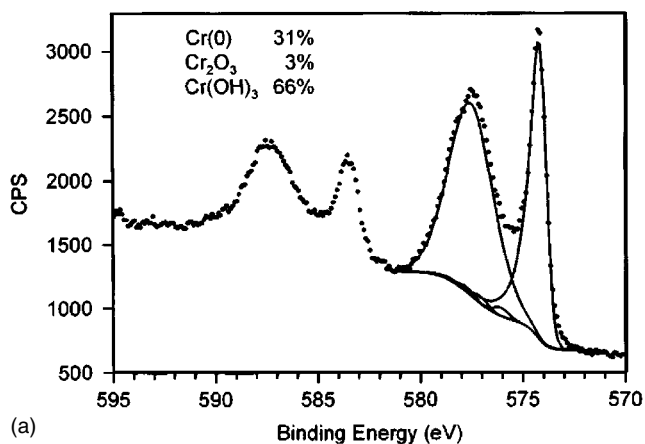


Figure 14. Chromium 2p spectrum for a chromated, zinc-galvanized steel. Spectrum is charge-corrected to O 1s ($\text{Cr}(\text{OH})_3$) at 531.7 eV. Fitting details are presented in the text.

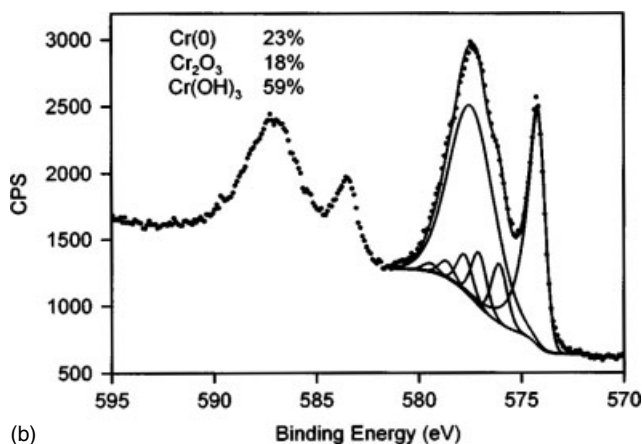
It is possible, but unlikely, that such peaks result from reconstruction of the outermost oxide layer(s). Rather, the peaks may be the result of near-surface point defects or dislocations associated with local mechanical strains in the structure.¹³ The broadened spectra that are characteristic of a number of the chromium compounds investigated also

present a challenge to rationalize: charge broadening is one explanation, but the consistency of the peak widths and positions observed would suggest a cause more associated with the material itself. Also, other spectra (C 1s, O 1s, etc.) from these samples are not broadened to any extent. The change in width of the Cr_2O_3 Cr 2p spectrum with *in situ* heat treatment (Figs 2 and 3) might result from dehydration of the polycrystalline structure, but no parallel change was found for other chromium compounds (CrF_3 , $\text{Cr}(\text{OH})_3$) following heat treatment (although CrF_3 may contain significant chromium oxide impurities: 5–10 at.% oxygen; see Table 1). Broadened structure was also found in the spectra of air-aged Cr_2O_3 (3 months, not shown). Also of note is the fact that hydrated specimens such as $\text{Cr}(\text{OH})_3 \cdot x\text{H}_2\text{O}$, $\text{CrB}_3 \cdot 6\text{H}_2\text{O}$, $\text{Cr}_2(\text{SO}_4)_3 \cdot x\text{H}_2\text{O}$ and $\text{CrPO}_4 \cdot 4\text{H}_2\text{O}$ (Figs 4, 10, 12 and 13, respectively) all show broad Cr 2p peak shapes. Finally, other unknown factors that can limit the achievement of higher spectral resolution, even in the presence of monochromatic x-radiation and good charge control, may be present.

The spectral fine structure observed for several of the well-resolved Cr(III) compounds does, in fact, bear a striking resemblance to the Cr(III) free ion structure calculated by Gupta and Sen.^{5,6} There are, however, small but measurable changes to the magnitude of the splitting, e.g. for the sesquioxide and sesquisulphide of chromium. Somewhat



(a)



(b)

Figure 15. Chromium 2p spectra of a decorative chrome-plated surface before (a) and after (b) a surface cleaning treatment. Note the increase in oxide after treatment. Fitting details are presented in the text.

more noticeable are the changes to the relative intensity of the multiplet components, e.g. between the chloride and oxide of Cr(III).

Beyond an examination of multiplet effects, this work has improved the definition of a number of Cr(III) species, some of which are important to the understanding of surface chemical passivation by chromium oxides, as well as the processes involving the deposition of thin Cr(III) oxide films from aqueous chromate solutions. The spectral BEs and peak widths for compounds such as Cr₂O₃, Cr(OH)₃ and the CrO₄²⁻ anion are key parameters to determining the presence of chromate on process surfaces. An example of this is shown

in Fig. 14, where the surface of a chromated, zinc-galvanized steel was analysed by XPS; the Cr 2p spectrum was obtained using the same high-resolution spectral conditions as above. In many cases, a thick zinc oxide was present at the surface and the use of the charge neutralizer was warranted. Additionally, poor electrical contact of the adventitious carbon overlayer with the chromated surface was found for many of the samples, making the use of adventitious carbon for charge correction impracticable. Processing conditions suggested that the bulk of the oxygen species are present as the hydroxide with a smaller lattice oxide contribution. Charge correcting to the O 1s hydroxide peak at 531.7 eV

Table 7. Summary of Cr 2p_{3/2} values for this work and average data from literature references

State/type of compound	Binding energy (eV) from this work ^a	SD (±eV)	Binding energy (eV) from literature average	SD (±eV)	Number of refs ^b
Cr(O)/Metal	574.2	—	574.2	0.3	15
Cr(III)/Cr ₂ O ₃	576.8 (576.9) [576.4]	0.1 (0.1) [0.2]	576.5	0.3	24
Cr(III)/Cr(OH) ₃	577.3	—	577.2	0.2	3
Cr(III)/CrF ₃	580.1	0.1	579.6	0.6	3
Cr(III)/CrCl ₃	577.7 (577.8) [577.5]	0.3 (0.3) [0.3]	577.6	0.3	2
Cr(III)/CrBr ₃	576.9	—	576.2	—	1
Cr(III)/Cr ₂ S ₃	574.8 (574.9) [574.6]	—	575.1	0.4	2
Cr(III)/Cr ₂ (SO ₄) ₃	578.5	—	—	—	0
Cr(III)/CrPO ₄	577.9	—	578.3	—	1
Cr(VI)/CrO ₃	—	—	579.2	0.7	5
Cr(VI)/(CrO ₄) ²⁻	579.0	0.1	579.5	0.6	10
Cr(VI)/(Cr ₂ O ₇) ²⁻	—	—	579.6	0.2	9
All Cr(VI)	—	—	579.5	0.5	24

^a Single peak-fit Cr 2p_{3/2} value, with weighted average of all multiplets in parentheses and weighted average of first two multiplets in square brackets. ^b Entries in NIST XPS database.¹⁴

Table 8. Summary of BE values for this work and average data from literature references (M = metal)

Photoelectron, type of compound	Binding energy (eV) from this work	SD (±eV)	Binding energy (eV) from literature average	SD (±eV)	Number of refs ^a
O 1s, Cr ₂ O ₃	530.2	0.2	530.3	0.3	13
O 1s, CrO ₃	530.1	—	530.2	0.6	3
O 1s, MOH	531.7 (M = Cr)	0.1	531.2	0.6	47
O 1s, FeCr ₂ O ₄	530.3	0.2	—	—	0
O 1s, NiCr ₂ O ₄	530.2	0.1	—	—	0
O 1s, M(Cr ₂ O ₇)	—	—	530.3	0.3	6
O 1s, M(CrO ₄)	—	—	530.1	0.5	8
O 1s, PbCrO ₄	530.1	—	—	—	0
F 1s, CrF ₃	685.7	0.1	685.5	—	1
Cl 2p _{3/2} , CrCl ₃	199.5	0.3	—	—	0
Br 3d _{5/2} , CrBr ₃	69.4	—	—	—	0
S 2p _{3/2} , Cr ₂ S ₃	161.4	—	162.7	—	1
S 2p _{3/2} , Cr ₂ (SO ₄) ₃	169.5	—	—	—	0
P 2p, CrPO ₄	133.7	—	133.4	—	1
Pb 4f _{7/2} , PbCrO ₄	138.6	—	138.8	—	1

^a Entries in NIST XPS database.¹⁴

(based on O 1s spectra for Cr(OH)₃; Table 5) was used. The Cr 2p peak was then fit with the multiplet splitting structure for Cr₂O₃ (BEs and weightings defined in Table 3), with a broad (2.5 eV) peak envelope for Cr(OH)₃ at 577.5 eV (similar to aged Cr(OH)₃ in Table 4) and a narrower peak at 579.5 eV indicative of a mix of Cr(VI) species. By using these charge correction procedures and fitting parameters, a variety of process conditions and treatments for a series of samples were consistently characterized with good results.

A second example involves a well-behaved decorative chrome-plated surface that has been treated to clean its surface. The untreated surface showed a well-defined metallic peak and a hydroxide peak (Fig. 15(a)). After the cleaning treatment, a well-defined metallic peak, a hydroxide peak and a contribution from Cr₂O₃ are seen in the resulting Cr 2p spectrum (Fig. 15(b)). The metallic peak is fitted with an asymmetric line shape defined by a sputtered chromium metal spectrum taken under the same analyser conditions. The oxide/hydroxide region uses the multiplet split peak shape and BEs defined earlier (see Table 2) for fresh Cr₂O₃ and a broad single peak (FWHM of 2.5 eV) for Cr(OH)₃ at 577.3 eV (fresh Cr(OH)₃ from Table 4). The resulting fit quite satisfactorily defines the species present.

Finally, the BE data for Cr 2p_{3/2} and O 1s spectra for the compounds studied are summarized in Tables 7 and 8 and compared with the best values obtained in earlier work.¹⁴ Further improvements to precision must await the

development of a charging reference procedure that uses a more reliable compound than adventitious carbon.

Acknowledgements

The authors would like to thank Dr M. Suominen-Fuller for her help with the MEM calculations and Ms R.J. Schuler for her preparation of the chromium hydroxide. The authors also would like to thank the Royal Ontario Museum (ROM) for donation of the eskolaite, chromite and crocoite minerals.

REFERENCES

1. McIntyre NS, Zetaruk DG. *Anal. Chem.* 1977; **49**: 1521.
2. McIntyre NS, Cook MG. *Anal. Chem.* 1975; **47**: 2208.
3. Ünveren E, Kemnitz E, Hutton S, Lippitz A, Unger WES. *Surf. Interface Anal.* 2004; **36**: 92.
4. Ilton ES, deJong WA, Bagus PS. *Phys. Rev. B* 2003; **68**: 125 106.
5. Gupta RP, Sen SK. *Phys. Rev. B* 1974; **10**: 71.
6. Gupta RP, Sen SK. *Phys. Rev. B* 1975; **12**: 15.
7. <http://www.casaxps.com>.
8. Splinter SJ, McIntyre NS. *Surf. Interface Anal.* 1998; **26**: 195.
9. Swaddle TW, Lipton JH, Guastalla G, Bayless P. *Can. J. Chem.* 1971; **49**: 2433.
10. Castle JE, Salvi AM, Guascito MR. *Surf. Interface Anal.* 1999; **27**: 753.
11. Miller DJ, Biesinger MC, McIntyre NS. *Surf. Interface Anal.* 2002; **33**: 299.
12. Grosvenor AP, Kobe BA, MC Biesinger, McIntyre NS. *Surf. Interface Anal.* 2004; in press.
13. Pratt AR, McIntyre NS, Splinter SJ. *Surf. Sci.* 1998; **396**: 266.
14. <http://srdata.nist.gov/xps/>.